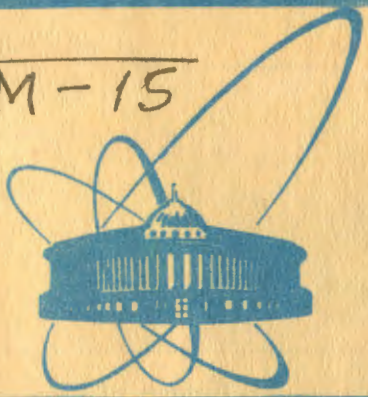

сообщения
объединенного
института
ядерных
исследований
дубна

E4-81-628

P.Mädler, L.Oehme,* R.Reif,* R.Wolf*

PREEQUILIBRIUM ANGULAR DISTRIBUTIONS IN (N, 2N) REACTIONS

* Technische Universität Dresden, Sektion Physik
8027 Dresden, DDR

1981

1. Introduction

In $(N,2N)$ reactions (N : nucleon) various nonstatistical effects are well established for incident energies between about 10 MeV and 100 MeV. In general, the single spectra and particle-particle angular correlations observed in $(p,2p)$ and $(p,p'n)$ processes have been interpreted in impuls approximation or distorted wave impuls approximation[1,2], assuming a quasielastic three-body knock-on collision as the dominating mechanism (see also[3] for a recent overview). On the other hand, the hybrid model for the preequilibrium decay of the compound system has been used, to remove the discrepancies between predictions based on an evaporation approach and measured excitation functions of $(n,2n)$ reactions[4-6].

The present paper contains some extension of previous work[7-9] on angular distributions of preequilibrium reactions in order to account for processes with two nucleons in the final channel, too. First, the generalized exciton model with momentum dependent partial state densities is applied for a $(N,2N)$ reaction, supposing statistically independent emission of both nucleons at different stages of the equilibrating process. Second, DWBA calculations with the excited nucleon occupying final states in the continuum are performed in order to estimate emission spectra and angular distributions, if only one particle is observed in the experiment. It is concluded, that both approaches may serve as a starting point to estimate preequilibrium effects in $(N,2N)$ reactions.

2. Generalized Exciton Model

The precompound model developed in[7] for a treatment of angular distributions in the framework of the exciton model allows an extension for $(N,2N)$ reactions. In this approach a two-step mechanism is assumed, in which both nucleons are emitted statistically

independent from exciton states $n=(p,h)$ and $n'=(p',h')$, separated by a certain number of steps k in the intranuclear cascade, which generates a chain of many particle (p) - many hole (h) states with growing complexity up to the compound nucleus. Then, the probability $W_{(ph)(p'h')}(\varepsilon_1,\Omega_1,\varepsilon_2,\Omega_2)$ for emitting two particles with definite kinetic energy $\varepsilon_1,\varepsilon_2$ and direction Ω_1,Ω_2 from the equilibrating system is a product of two probabilities

$$W_{(p,h)(p';h')}(\varepsilon_1,\Omega_1,\varepsilon_2,\Omega_2) = W^{(1)}_{(p,h)\to(p-1,h)}(\varepsilon_1,\Omega_1)\,W^{(2)}_{(p;h')\to(p'-1,h')}(\varepsilon_2,\Omega_2) \quad (1)$$

with $p'=p-1+K$, $h'=h+K$. For $k=0$, one has two successive emissions from a given exciton state, implying a double direct mechanism $(2p,1h)\to(1p,1h)\to(0p,1h)$ for the preequilibrium decay of the state with initial exciton number $n_0=3$. In eq. (1) each emission probability $W^{(m)}$ is determined by the ratio of the partial densities of states $\varrho_{p,h}(E,\vec{P})$ with p particles and h holes in the initial and final state of the reaction step with total energy E and total linear momentum $\vec{P}$, both counted from the center of the Fermi sphere. Then, in the spirit of the exciton model[10] the multi-differential cross section of a $(N,2N)$ reaction can be written as

$$\frac{\partial^4\sigma}{\partial\varepsilon_1\partial\Omega_1\partial\varepsilon_2\partial\Omega_2} \sim \varepsilon_1\,\varepsilon_2\,\sigma^{(1)}_{inv}(\varepsilon_1)\,\sigma^{(2)}_{inv}(\varepsilon_2)\times \quad (2)$$

$$\sum_{h=1}^{\bar{h}} \frac{\varrho_{p-1,h}(U_1,\vec{P}_1)}{\varrho_{p,h}(E,\vec{P})} \sum_{k=0}^{\bar{k}-b} \frac{\varrho_{p'-1,h'}(U_2,\vec{P}_2)}{\varrho_{p';h'}(U_1,\vec{P}_1)} \quad ; \quad p=h+1,\ h'=h+k=p'.$$

Here $\sigma^{(m)}_{inv}(\varepsilon_m)$ denotes the inverse cross section, and E,U_1,U_2 and $\vec{P},\vec{P}_1,\vec{P}_2$ are the total energy and the total linear momentum of the exciton gas before, after the first, and after the second nucleon emission, respectively.

The recoil of the residual nucleus after the first emission can be taken into account by shifting the Fermi sphere by $\Delta\vec{P}=(\vec{P}_c-\vec{P})/A$ with $\vec{P}_c$ and A denoting the total linear momentum of the compound system in the laboratory frame and the number of the nucleons in the non-excited core, respectively. Such a recoil effect has to be included in the kinematic relations for U_1,U_2 and $\vec{P}_1,\vec{P}_2$. Then, with these values the relevant densities appearing in eq. (2) can be determined numerically (see ref.[10]).

It should be emphasized, that distortion effects are not taken into account within this model. This fact could turn out to be a shortcoming, if one wants to explain properties of particle-particle correlations.

3. Double Differential Cross Section in DWBA

A DWBA calculation allows for a reasonable description of preequilibrium effects in the differential cross section of medium energy inelastic nucleon-nucleus scattering processes at higher excitation[8,9], in particular, if second order effects are included[11]. In such an approach the total strength for a one-step transition with given energy loss and angular momentum transfer is composed incoherently out of single particle excitations with the excited nucleon occupying bound single particle states in the shell model potential of the target. On the same footing, the contribution of the $(N,2N)$-channel on the precompound nucleon emission spectra and angular distribution can be estimated. This extension can be performed by assuming a mechanism, in which a single interaction between the incoming nucleon and the struck nucleon of the target promotes the latter to a final state in the continuous part of the single particle spectrum, with the projectile remaining in an unbound state. Such a model consideration starts from the standard DWBA matrix element

$$T_{fi} = \langle \chi^{(-)}_{\vec{k}_{p'}}(\vec{r}_{p'}) \left| \left(\chi^{(-)}_{\vec{k}_n}(\vec{r}_n)\, \phi_{I'M'}(A) \left| V_{np} \right| \phi_{IM}(A+1) \right) \right| \chi^{(+)}_{\vec{k}_p}(\vec{r}_p) \rangle . \quad (3)$$

The initial state i contains a proton of momentum $\hbar\vec{k}_p$ and a target of $A+1$ particles in a state $\phi_{IM}(A+1)$ with spin quantum numbers I,M. The neutron-proton interaction V_{np} leads to a final state f, which consists asymptotically of a residual nucleus in a state $\phi_{I'M'}(A)$, an outgoing proton with momentum $\hbar\vec{k}_{p'}$, and an ejected neutron with momentum $\hbar\vec{k}_n$. From energy conservation one has $E_p = E_{p'} + E_n + B_n(A+1)$ (B_n : neutron separation energy in the target).

In order to simplify the calculations the target ground state is assumed to consist of a neutron in a single particle state $\varphi_{nljm} = \frac{U_{nlj}(r_n)}{r_n}\left[Y_l(\Omega_n)\chi_s \right]_{jm}$ bound to an infinitely heavy spinless core $|0\rangle$, which does not participate in the reaction. So, one has the target wave function $\phi_{IM}(A+1) = \varphi_{nljm}|0\rangle\delta_{Ij}\delta_{Mm}$ and the probability for separating a neutron from the target ground state, which corresponds to the spectroscopic factor of a (p,d) pick-up reaction, becomes unity.

The two-nucleon state in the final channel is described as a product of two scattering waves, which are generated from distorting potentials U_p, U_n, expressing the overall interaction of the

nucleon emitted with the residual nucleus. This approximation implies the assumption, that the outgoing nucleons are not correlated in the final channel. This holds, if the relative motion of the neutron and proton is mainly determined by the seperate action of the mean potentials U_p, U_n, rather than by the mutual two-body interaction v_{np}.

Furthermore, the re-absorption of the neutron after leaving the bound orbit is neglected, and both the continuum wave function $\chi^{(-)}_{\vec{k}_n}(\vec{r}_n)$ and the bound state wave function φ_{nljm} of the neutron are computed in the same real Woods-Saxon potential. Consequently, in a partial wave decomposition of $\chi^{(-)}_{\vec{k}_n}(\vec{r}_n)$ the phase shift in the asymptotic form of the radial wave function $w_{l'j'}$ is real, and real form factors can be used in the DWBA calculation of the partial transition amplitudes.

After a multipole expansion of the effective interaction

$$v_{np} = \sum_{LM} g_L(r_n, r_p)\, Y_{LM}(\hat{r}_n)\, Y^*_{LM}(\hat{r}_p) \qquad (4)$$

the inner matrix element can be evaluated. In order to simplify the angular momentum algebra involved, the neutron is supposed to be bound in a s-state. Then, the angular momentum L transferred in the two-body interaction coincides with the angular momentum l' carried by the ejected neutron. Finally, the form factor appearing in the inner matrix element of eq. (3) (for definition and notation see ref. /12/) can be expressed in terms of radial integrals

$$I_{l'j'}(r_p) = \int dr_n\, w_{l'j'}(r_n)\, g_{l'}(r_n, r_p)\, U_{s_{1/2}}(r_n). \qquad (5)$$

In computing this radial integrals no probleme of convergence appear, because in the asymptotic region the oscillations of the continuum wave function are cut off by the exponential decay of the bound neutron wave function.

In a single-counter experiment the neutron is not detected. Thus, the multi-differential cross section $d^3\sigma/dE_{p'}\,d\Omega_{p'}\,d\Omega_n \sim |T_{fi}|^2$ has to be integrated over the direction Ω_n of the emitted neutron. In this way interference terms between contributions with different $l'j'$ disappear because of the orthogonality of the spherical harmonics $Y_{l'\lambda}(\hat{k}_n)$ involved in the partial wave decomposition of $\chi_{\vec{k}_n}(\vec{r}_n)$. As a final result one obtains the double differential cross section as a sum of partial cross sections for various neutron transitions $2s_{1/2} \longrightarrow l'j'$

$$d^2\sigma/dE_{p'}\,d\Omega_{p'} = \sum_{l'j'} d^2\sigma(l'j')/dE_{p'}\,d\Omega_{p'} \qquad (6)$$

which can be evaluated using a standard DWBA code, with the phase space factor taken from ref. /13/. From eq. (6) one derives the proton emission spectrum by integrating $\Omega_{p'}$. It is decomposed according to different multipolarity of single particle transitions, so that apart from the phase space factor the general behaviour is determined by the single particle structure of the continuum.

Similar theoretical investigations as presented in this paper have been reported by Yezhov et al. /14-16/ for the excitation function, the particle emission spectra, and the particle-particle angular correlations in $(n,2n)$ reactions on various targets (Pb, Bi, Co, Fe, Zn) for incident energies in the range of 10-20 MeV. Good agreement with experimental data could be obtained. But the angular distribution of emitted neutrons has not been discussed in this series of papers. In this context it should be mentioned that in most of the calculations of Yezhov et al., some further simplifications as square well distorting potentials and zero-range effective forces have been introduced. Such approximations should be not too severe as one looks for excitation functions and spectra. But, keeping in mind the widely accepted experience in applying a microscopic description to inelastic nucleon scattering, these oversimplifications could become questionable, if one emphasizes the prediction of angular distributions.

4. Numerical Results and Discussions

As an example the reaction $^{29}Si(p,p'n)^{28}Si_{g.s.}$, $E_p = 30\,MeV$ has been chosen, in which the neutron is ejected from a $2s_{1/2}$ orbit. The numerical calculations have been performed with the code DWUCK. The radial wave functions of the neutron in the bound as well as in the scattering states were computed in a real Woods-Saxon potential with the shape parameters $r = 1.27$ fm, $a = 0.67$ fm and the spin-orbit coupling strength $V_{ls} = 8.5028$ MeV given in /17/. The potential depth $V_0 = 47.925$ MeV is adjusted to reproduce the experimental neutron seperation energy $B_n = -8.5$ MeV. The parameters of the optical potential (real Woods-Saxon term, surface absorption of Woods-Saxon derivative type) for the proton channels are taken from /18/. For the strength and the range parameter of the effective Yukawa interaction V_{np} the standard values $V = 100$ MeV and $\mu = 1.0$ fm have been inserted. In the sum of equation (6) transferred angular momenta up to $l' = 6$ must be taken into account, while for higher l' values the overlap of the continuum and the bound state neutron wave functions decreases rapidly with increasing l'.

4.1. Transition form factors

The shape of the transition form factors, which localizes the reaction and therefore determines the amount of the diffractional structure of the angular distributions, is expressed in terms of the radial integrals (5) as a function of the proton coordinate r_p. The behaviour of the radial integrals in space and the absolute magnitude of it is directed by the overlap of the oscillating scattering radial wave function w and the bound state wave function v, confined mainly within the range of $r_n \lesssim 10$ fm. The radial integrals strongly depend on the transferred angular momentum, and on the neutron energy in the continuum. As an example, numerical results for the transition form factors are presented in fig. 1 for the transitions $2s_{1/2} \longrightarrow p_{1/2}$, $2s_{1/2} \longrightarrow g_{9/2}$.

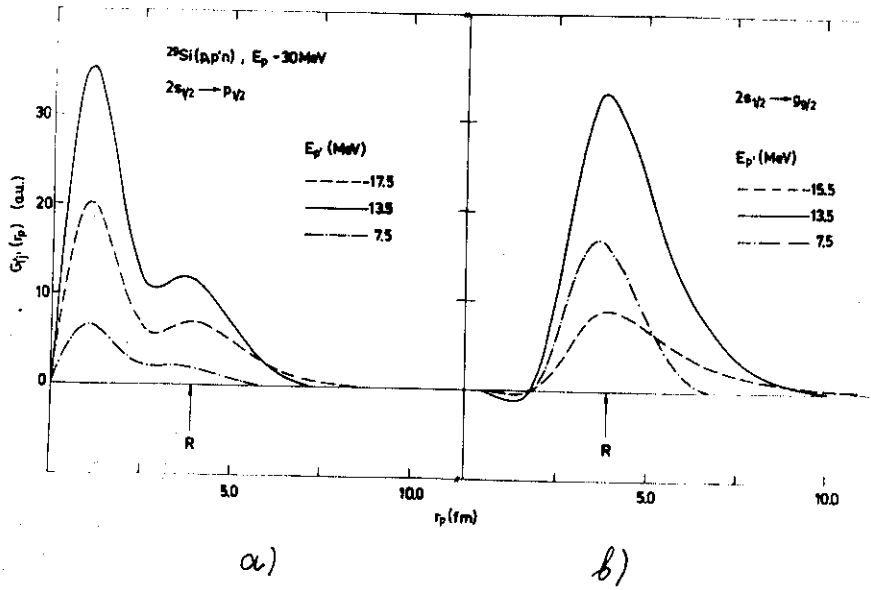

Fig. 1. DWBA form factor $G_{l'j'}(r_p)$ of the neutron transitions $2s_{1/2} \longrightarrow p_{1/2}$ (a) and $2s_{1/2} \longrightarrow g_{9/2}$ (b) in the reaction $^{28}Si(p,p'n)$, $E_p = 30MeV$ for various proton emission energies $E_{p'}$. R: nuclear radius.

For low transferred angular momentum ($l=0,1$) the knock-on preferrentially proceeds in the interior region of the target. If the orbital angular momentum of the neutron is large enough ($l \geq 4$), the scattering wave functions show a smooth increase with increasing r_n for the region, in which the bound state wave function is localized. Thus, the transition form factor shows only a broad maximum near the nuclear radius. The situation is more complex for partial waves in between ($l=2,3$), for which the continuum wave function starts to oscillate inside the nuclear radius, leading to a more complicated shape of the form factor, with two nodes in some cases.

The striking feature of the energy dependence of the transition form factor is the regular resonance behaviour connected with the occupation of single particle resonances in the continuum of excited neutron states. If the neutron energy is varied, the magnitude of the transition form factor changes drastically, while the main characteristics of the shape are preserved for most of the partial waves considered.

4.2. Proton emission spectra

The partial proton emission spectra exhibit a pronounced resonance structure (see fig. 2). For S- and P-waves three broad resonances appear in the energy range considered, with a half width of about 5 MeV and a spacing of about 8-10 MeV. The spin-orbit splitting of the position of the resonances with $j = l \pm 1/2$ amounts up to about 4 MeV. In the single particle resonances the angle integrated partial cross section reaches an upper value in the order of 1 mb/MeV, which is comparable to the calculated inelastic scattering cross section for the single particle excitation to the bound state. Between the resonances the partial cross section is lower by several orders of magnitude. This result supports the conclusion drawn in /19/ in the analysis of $(\alpha,\alpha'N)$ reactions on ^{12}C and ^{16}O at 175 MeV with projecting out from the continuum wave function a single particle bound state and an orthogonal rest-continuum. Comparing with experiment, it was found in this paper, that about 20% (3 mb/sr MeV) of the observed cross section comes from the knock-on reactions to the resonant continuum, the non-resonant contribution being negligibly small.

In the summed spectrum the relative contribution of different partial waves depends on the proton emission energy. The low partial waves ($l'=0,1,2$) are dominating in the high energy region ($E_{p'} \approx$ 18-20 MeV) as it is expected from the fact, that the knock-on mechanism should favour small momentum transfer. On the other

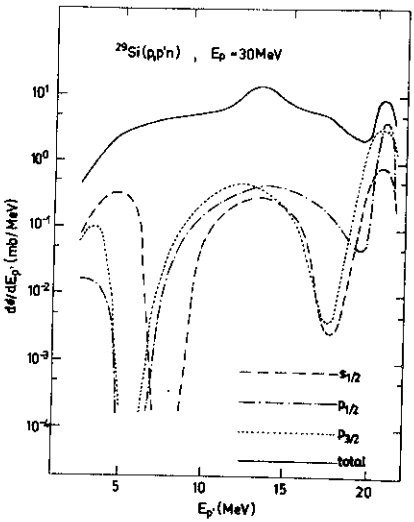

hand, in the low energy region ($E_{p'} \approx 3$-5 MeV) processes with $l' = 5,6$ are slightly preferred, while in the intermediate range ($E_{p'} \approx 10$ MeV) nearly all partial waves contribute to the emission spectrum. The structure predicted near $E_{p'} \approx 20$ MeV is connected with s- and p-resonances, while the small bump at $E_{p'} \approx 12$ MeV can be assessed to a g-resonance.

Fig. 2. Partial contribution of transferred angular momenta $l_j = s_{1/2}, p_{1/2}, p_{3/2}$ to the total proton emission spectrum (solid line) in the reaction $^{29}Si(p,p'n)$, $E_p = 30$ MeV calculated in DWBA.

4.3. Angular distribution

The angular distributions of the emitted protons show a marked dependence on angular momentum and, in particular, on the emission energy. This holds for the partial differential cross section (figs. 3,4) as well as for the summed differential cross section (fig. 5).

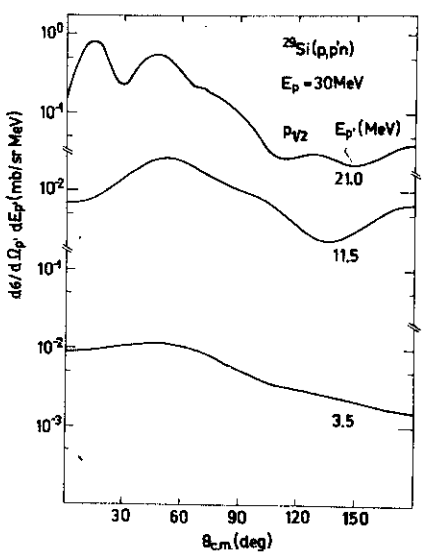

Fig. 3. Reaction $^{29}Si(p,p'n)$, E_p =30MeV. Double differential cross section for transferred angular momentum $l = 1, j = 1/2$ for various proton emission energies $E_{p'}$, calculated in DWBA.

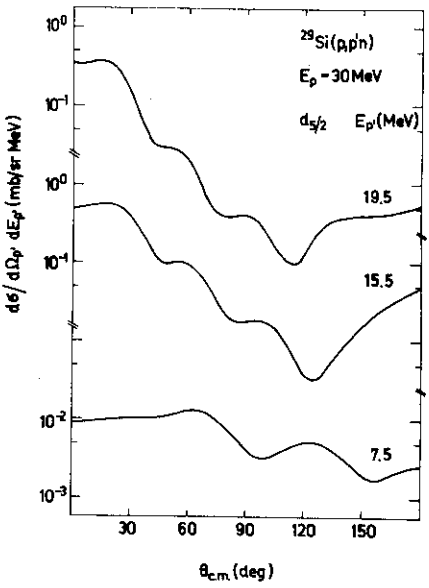

A general tendency in the behaviour of the shape of the angular distribution is the transition from a forward peaked, more diffraction like pattern at high emission energies to a more smooth curve for low emission energies. For high transferred l'values and high emission energies the proton leaves the interaction region within a rather narrow range of reaction angles, which is shifted slightly to larger values if l'increases.

Fig. 4. Reaction $^{29}Si(p,p'n)$, E_p = 30 MeV. Double differential cross section for transferred angular momentum $l = 2$, $j = 5/2$ for various proton emission energies $E_{p'}$, calculated in DWBA.

The diminishing of the forward-backward asymmetry with decreasing proton emission energy results mainly from the Q-value dependence of the DWBA matrix element. So, the ratio of the summed differential cross section in the forward and backward region decreases by a factor of more than 4, if $E_{p'}$ is lowered from 21.0 MeV to 3.5 MeV. If in extended calculations the ejection of the neutron out of more than one bound state with

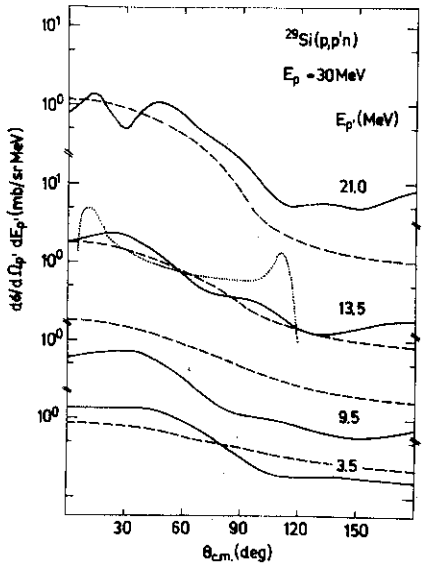

Fig. 5. Double differential cross section of the reaction $^{29}Si(p,p'n)$, E_p=30 MeV for various proton emission energies. Solid line: DWBA. Dashed line: predictions of the generalized exciton model[7] for the (p,p') reaction, normalized for an emission energy of $E_{p'}$ = 21 MeV at forward angles. Dotted curve: double direct reaction to the ground state, eq.(2). The curve has been normalized independently.

$L \neq 0$ would come into play, the angular momentum algebra involved becomes more complex, and interference effects between different transitions could change the general picture.

4.4. Generalized exciton model

In fig. 5 the DWBA angular distributions of the $(p,p'n)$ reaction are compared with predictions of the generalized exciton model of ref./7/ applied for a (p,p') process. The basic difference between both calculations comes from the fact, that the exciton model does not distinguish between final $n = 2$ states containing a particle above the nucleon threshold or not. From fig. 5 it can be seen, that at higher emission energies the exciton model fails to reproduce the diffraction-pattern of the angular distributions, and the cross section is too small at backward angles. For lower emission energy the rather smooth shape of the angular distributions is reproduced only in the average. Furthermore, the exciton model is unable to follow the resonance behaviour of the cross section.

In order to demonstrate the application of eq. (2) the first term, which is expected to be the leading term, is investigated by restricting to ground state transitions. In this case the hole is fixed at the Fermi surface and the density of final states is replaced by a δ -function, containing the corresponding dispersion relation. For fixed kinetic energy and direction of the emitted proton, the following neutron emission is strongly restricted by the kinematical relations typical for a three-body reaction. So, only two very small intervals of the momentum of the emitted neutron contribute to the double differential cross section. The range of the intervals, corresponding to different positions of the hole at the Fermi surface in momentum space, is determined by the recoil of the final nucleus. Integrating the energy and direction of the emitted neutron, the double differential cross section for the proton emission, being very small at extrem forward angles, reaches a maximum for $\theta_p \approx 10°$ followed by a decrease similar to the results of the exciton model or the DWBA calculation (see fig. 5).

5. Conclusions

The methods proposed in this paper are suitable to estimate the influence of the $(N,2N)$ channel on the preequilibrium nucleon emission in nucleon induced reactions (spectra and angular distributions). For a $(p,p'n)$ reaction in a direct single scattering the elementary excitation of an initially bound neutron to a single particle state

in the continuum of the shell model potential proceeds with a probability, which is comparable with that for an inelastic transition to a final bound state. The shape of the proton emission spectrum and the strength of the angle integrated cross section are determined by the position and the width of the neutron single particle resonances contributing to various transferred angular momenta. With decreasing emission energy the angular distribution tends to lose the forward peaking as well as the diffractional structure. In more realistic calculations nuclear structure amplitudes are involved, determined by the continuum component of the target wave function in the final state. Further refinements of the calculations are recommended. So, an absorptive part should be included in the distorting potential U_n, which gives a complex form factor in the distorted wave matrix element. Furthermore, the formation of a deuteron as a transient state during the course of the reaction or the coupling to the (p,d) pick-up channel cannot be neglected completely. Also the investigation of particle-particle-correlations is possible by avoiding the integration of the direction of one ejected particle, leading to an angle dependent form factor.

For higher incident energies a DWBA approach takes much efforts, because higher-order effects are of importance and the residual nucleus may be left at high excitation. In this case a statistical description of the process in terms of energy and momentum dependent partial state densities (generalized exciton model) allows for a more simplified treatment.

References

1. Jackson D.F. Adv.Nucl.Phys., 1971, 4, p. 1.
2. Lim K.L., McCarthy I.E. Nucl.Phys., 1966, 88, p. 433.
3. Miller C.A. In: Proc. 9 th Int. Conf. on the Few Body Problem, Eugene, Oregon. Nucl.Phys., 1981, A353, p. 157c.
4. Seeliger D., Meister A., Seidel K. Yad.Fiz., 1976, 23, p. 745.
5. Holub E., Cindro N. Phys.Lett., 1975, 56B, p. 143.
6. Holub E., Cindro N. J.Phys. G: Nucl.Phys., 1976, 2, p. 405.
7. Mädler P., Reif R. Nucl.Phys., 1980, A337, p. 445.
8. Arndt E., Reif R. TU-Information, 05-32-76, Dresden, 1976.
9. Reif R. Acta Phys.Slov., 1975, 21, p. 208.
10. Griffin J.J. Phys.Rev.Lett., 1966, 17, p. 478.
11. Tamura T. et al. Phys.Lett., 1977, 66B, p. 109.
12. Satchler G.R. Nucl.Phys., 1966, 77, p. 481.
13. Baur G., Trautmann D. Phys.Rep., 1976, 25C, p. 294.

14. Yezhov S.N. et al. Yad.Fiz., 1970, 11, p. 22.
15. Yezhov S.N., Olkhovski V.S. Yad.Fiz., 1972, 16, p. 332.
16. Yezhov S.N., Plyuyko V.A. Yad.Fiz., 1978, 28, p. 83.
17. Bohr A., Mottelson B.R. Nucleare Structure. vol. I. Benjamin, New York, 1969.
18. Becchetti F.O., Greenless G.W. Phys.Rev., 1969, 182, p. 1190.
19. V.Geramb H.V., Nordland O. In: Proc. Int. Conf. on Nuclear Reaction Mechanism, Varenna, 1977, p. 299.

Received by Publishing Department
on October 1 1981.